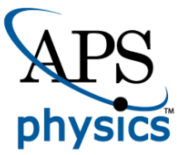

Dissipation-Assisted Coherence Formation in a Spinor Quantum Gas

Yujiro Eto, Hitoshi Shibayama, Kosuke Shibata, Aki Torii, Keita Nabeta, Hiroki Saito, and Takuya Hirano

Phys. Rev. Lett. **122**, 245301 — Published 21 June 2019

DOI: 10.1103/PhysRevLett.122.245301

Dissipation-assisted coherence formation in a spinor quantum gas

Yujiro Eto[1,2], Hitoshi Shibayama[3], Kosuke Shibata[4], Aki Torii[4], Keita Nabeta[4], Hiroki Saito[5], and Takuya Hirano[4]
[1]*National Institute of Advanced Industrial Science and Technology (AIST), NMIJ, Tsukuba, Ibaraki 305-8568, Japan*
[2]*JST, PRESTO, 4-1-8 Honcho, Kawaguchi, Saitama 332-0012, Japan*
[3]*College of Industrial Technology, Nihon University, Narashino 275-8576, Japan*
[4]*Department of Physics, Gakushuin University, Toshima, Tokyo 171-8588, Japan*
[5]*Department of Engineering Science, University of Electro-Communications, Chofu, Tokyo 182-8585, Japan*
(Dated: May 21, 2019)

We report the formation of magnetic eigenstates assisted by naturally occurring particle dissipation in a Bose–Einstein condensate of spin-2 ^{87}Rb atoms. Although the atomic interaction energetically favors the non-ferromagnetic state, we observed the spontaneous evolution of an unpolarized spin state into the transverse ferromagnetic state. Under such dynamics, the spin-dependent dissipation of atoms enhances the synchronization of the relative phases among five magnetic sublevels to promote magnetization. Through numerical simulations based on mean-field theory, we show that another exotic magnetic eigenstate, the cyclic state, can also be formed through the spin-dependent dissipation of atoms.

Clarifying the various effects of energy and particle dissipation coupling to the environment will lead to a deeper understanding of open quantum systems and will expand the applications of quantum physics. Dissipation often reduces the quantum coherence, which is a major problem in quantum information science, such as quantum computation and quantum simulation [1]. On the other hand, dissipation sometimes has the opposite effect of promoting quantum coherence, and such dissipation can be used as a new control strategy for quantum systems and as a useful resource for quantum computations [2]. Through proper design of the coupling between the system and the surrounding environment, it is possible to prepare a desirable pure quantum state in an open quantum system to explore quantum simulation using strongly correlated many body states [3]. The stabilization of entangled qubits in superconductor and atomic ions [4, 5] and the control of quantum phase transitions in cold atoms [6] have been experimentally demonstrated by exploiting controllable dissipation.

Beneficial effects of dissipation are also caused by uncontrollable naturally occurring dissipation. Natural dissipation has been used to protect quantum states in optical applications. Optical loss maintains a coherent state or brings other states closer to a coherent state [7]. Under such energy dissipation, photons are lost, but the phases between the photon-number bases are not randomized, enabling the transmission of light while maintaining the phase of the complex amplitude of the light field. Recently, prolonging the coherence time under natural dissipation has been discussed in biological systems to understand efficient processes in nature [8]. In photosynthetic systems, such an effect is related to efficient electron transport [9, 10].

In this Letter, we investigate the magnetization dynamics in dissipative Bose–Einstein condensates (BECs) of spin-2 (hyperfine spin $F = 2$) ^{87}Rb atoms. We experimentally observed the emergence of symmetry-breaking magnetization from an unpolarized spin state. Symmetry-breaking magnetization has been observed in a spin-1 ^{87}Rb BEC [13], in which the magnetization is induced by the ferromagnetic interactions between atoms. In contrast, in a spin-2 ^{87}Rb BEC [11], although the corresponding interactions are not ferromagnetic, the unpolarized spin state evolves into a transverse ferromagnetic state.

We found from the comparison of experimental and theoretical results that spin-dependent particle dissipation plays an essential role in the formation of a ferromagnetic state. In this system, the $F = 2$ state of ^{87}Rb atoms undergoes inelastic collisional loss, in which two $F = 2$ atoms collide and escape from the trap by a transition from the $F = 2$ state to the $F = 1$ states [12]. Although the total spin $\mathcal{F}$ of the two colliding $F = 2$ atoms can be $\mathcal{F} = 4$, 2, or 0, decay through the $\mathcal{F} = 4$ channel is prohibited by angular-momentum conservation, since the $F = 1$ state cannot participate in the $\mathcal{F} = 4$ channel. In other words, inelastic collisional loss of two atoms is suppressed when they are fully magnetized in the same direction. As a consequence, the magnetized state accumulates and is purified in the trap by the dissipation of other states. This magnetization dynamics is in stark contrast to the conventional dynamics, in which the spin vectors align in the same direction to lower the interaction energy [13].

A schematic of the observed spinor dynamics is illustrated in Fig. 1. We performed the experiments using a spin-2 BEC consisting of the five magnetic sublevels, $m = -2, -1, 0, +1$, and $+2$. The magnetization, S_i, along the i-axis was obtained from the population in each magnetic sublevel, $\rho_{m,i}$, with the i-axis as the quantization axis ($S_i = \Sigma_m m\rho_{m,i}$). The atoms were initially prepared in the $|F = 2, m = 0\rangle$ state with the quantization axis along a magnetic bias field on the z-axis. This state is the completely unpolarized spin state with rotational symmetry around the z-axis [Fig. 1(a)]. After time

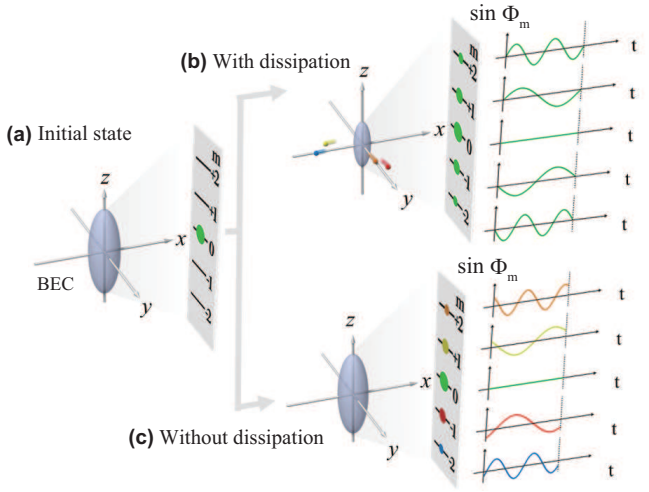

FIG. 1: Conceptual diagram of coherence formation assisted by spin-dependent particle dissipation. (a) The as-prepared unpolarized spin state of $|F = 2, m = 0\rangle$, where F and m are the quantum numbers for the total angular momentum and the Zeeman sublevel, respectively. The populations in the $|2, m\rangle$ states are depicted in the grey box. (b) and (c) show the spin states after time evolution with and without dissipation, respectively. The sinusoidal curves represent the phases $\sin\Phi_m = \sin(m\omega t + \phi_m)$, where ω is the linear Zeeman frequency under a magnetic field in the z-direction. The phase offset, ϕ_m, is expressed by different colors. The atoms populate all five components in both (b) and (c). The fully polarized transverse magnetization is generated only in a dissipative system, namely Φ_m obeys the relationship $\Phi_2 - \Phi_1 = \Phi_1 - \Phi_0 = \cdots = \Phi_{-1} - \Phi_{-2}$ due to the dissipation.

evolution, the atoms were distributed into all m components by two-body elastic collisions while preserving a longitudinal magnetization S_z of zero. Similar dynamics of $\rho_{m,z}$ have previously been investigated experimentally [14–16]. The most significant difference from the previous studies is that we also measured the transverse magnetization, $S_\perp = S\cos\alpha$, orthogonal to the z-axis, making it possible to obtain information on the phase coherence, where $S = \sqrt{S_x^2 + S_y^2}$ is the magnitude of the transverse magnetization and α is the azimuth angle of the spin vector. We found that the transverse magnetization is almost fully polarized, $S \simeq 2$, after time evolution. Transversely fully polarized state rotating on the $x - y$ plane is expressed by the two-axis rotation of the longitudinally fully polarized state as follows:

$$\hat{R}_z(\alpha)\hat{R}_y(\frac{\pi}{2})\,|m = 2\rangle = \frac{e^{-i2\alpha}}{4}\,|2\rangle + \frac{e^{-i\alpha}}{2}\,|1\rangle + \sqrt{\frac{3}{8}}\,|0\rangle + \frac{e^{i\alpha}}{2}\,|-1\rangle + \frac{e^{2i\alpha}}{4}\,|-2\rangle\,,$$

where the operator $\hat{R}_i(\theta)$ rotates the spin state around the i-axis by an angle θ. In such state, the phases in the magnetic sublevels, Φ_m, satisfy $\Phi_2 - \Phi_1 = \Phi_1 - \Phi_0 = \Phi_0 - \Phi_{-1} = \Phi_{-1} - \Phi_{-2}$. Therefore, the generation of the transverse magnetization with $S \simeq 2$ implies the formation of phase coherence. The atoms distributed in the five m components therefore acquire phase correlation, and the phases rotate with the Zeeman frequency synchronously [Fig. 1(b)]. On the other hand, phase synchronization does not occur in a numerical simulation without dissipation [Fig. 1(c)]; thus, it can be concluded that the phase synchronization is due to dissipation.

We used a BEC trapped in a crossed far-off-resonance optical trap (FORT). The axial and radial frequencies of the FORT are $\omega_z/(2\pi) = 64$ Hz and $\omega_r/(2\pi) = 190$ Hz, respectively. The external magnetic field of $B_z = 200$ mG is aligned with the axis of the trap (z direction), which produces a quadratic Zeeman shift, $|q|/h \simeq 3$ Hz. The pure $|2, 0\rangle$ state is produced from the state occupying the multiple m levels by using microwave pulses and a blasted beam [see Supplemental Material (SM)]. The purity of the $|2, 0\rangle$ state in this study was greatly enhanced relative to that in our previous experiment [16], to remove other components. The BEC prepared in the $|2, 0\rangle$ state was then held in the optical trap for a variable time of $T_{\rm hold}$. To measure S_z, the BEC was released from the trap, and each m component was spatially separated along the z direction using the Stern-Gerlach method. On the other hand, to measure $S_\perp$ orthogonal to the z direction, we irradiated the BEC with a $\pi/2$ radio frequency (rf) pulse just before releasing it from the trap. The $\pi/2$ rf pulse effectively rotated the measurement axis by $\pi/2$. After a time of flight for 15 ms, the spatial distribution of each m component was measured using absorption imaging. The number of atoms in each m component was estimated by performing the bimodal fitting of the atomic distribution. The longitudinal or transverse magnetization per atom, S_i, was calculated from $\rho_{m,i}$.

We first experimentally investigate the spinor dynamics along the longitudinal axis (z-axis). Figure 2(a) shows the dependence of $\rho_{m,z}$ on the free-evolution time, $T_{\rm hold}$. The $m = \pm1$ components grow after $T_{\rm hold} \simeq 30$ ms, followed by a delayed growth in the $m = \pm2$ components after $T_{\rm hold} \simeq 50$ ms. The initial slow rise of the $m = \pm1$ components in Fig. 2(a) reflects the metastability of the $m = 0$ state [14, 17]. Indeed, in the case where the initial state includes components other than the $m = 0$ state, the initial change is faster (see SM). The longitudinal magnetization, S_z, calculated from the results shown in Fig. 2(a) remains almost stable around zero, as shown in Fig. 2(b). As shown in the inset of Fig. 2(a), the total number of atoms is reduced, mainly due to spin-dependent particle dissipation by inelastic collisional loss. The degree of loss by other processes such as photon scattering from the dipole trap was estimated using the $|2, -2\rangle$ state, which is immune to inelastic collisional loss [18]. In this case, the total loss of atoms at $T_{\rm hold} = 150$ ms is less than 10%.

We next investigate the dynamics of $S_\perp$. As for the dynamics measured along the z-axis, no change is seen up to

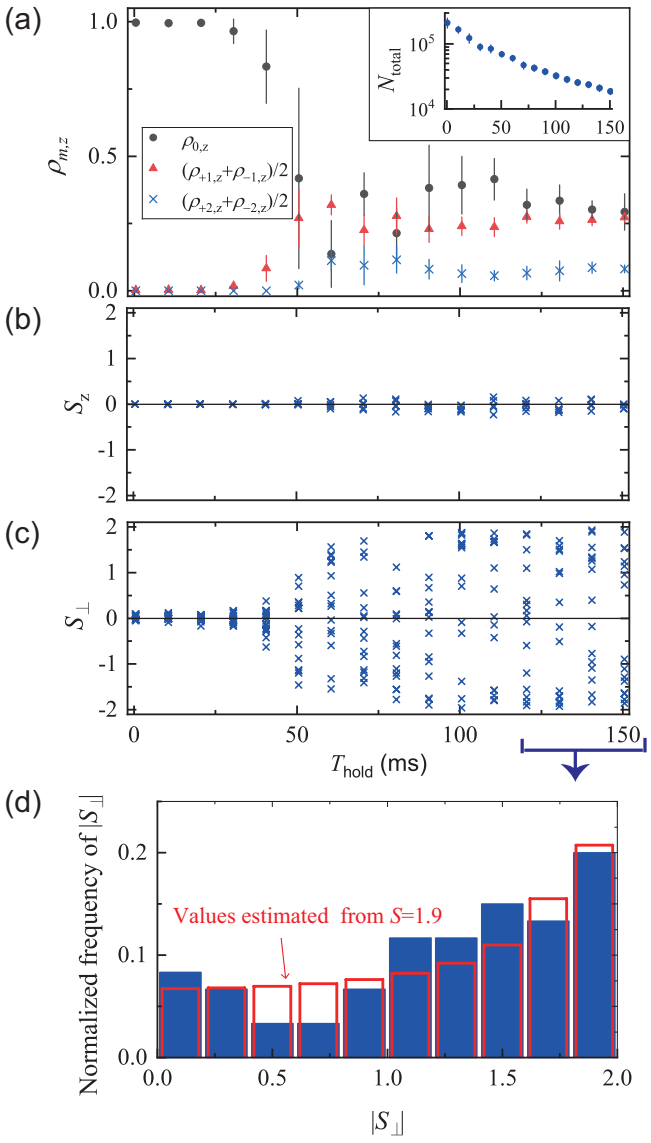

FIG. 2: Observation of the spinor dynamics starting from an unpolarized spin state $|2,0\rangle$. (a) Time evolution of the populations $\rho_{m,z}$ in the magnetic sublevels m. The inset shows the total number of atoms. (b) Dynamics of the longitudinal magnetization, S_z. (c) Dynamics of the transverse magnetization, $S_\perp$. (d) Normalized occurrence distribution of $|S_\perp|$ obtained during $T_{\rm hold}$ = 120 - 150 ms. The histogram with a bin width of 0.2, was constructed from 60 experimental data points in (c), and the red empty histogram indicate the fitting results.

$T_{\rm hold} \simeq 30$ ms. However, unlike for the dynamics of $\rho_{m,z}$, the shot-to-shot variations in $\rho_{m,\perp}$ for each $T_{\rm hold}$ greatly increase after $T_{\rm hold} \simeq 30$ ms, which results in $S_\perp$ varying between -2 and $+2$, as shown in Fig. 2(c). We now consider the cause of the shot-to-shot variations in $S_\perp$ observed in Fig. 2(c). Since the initial $m = 0$ state has rotational symmetry around the z-axis, the occurrence of transverse magnetization should be a consequence of spontaneous breaking of the rotational symmetry. Therefore, the azimuth angle of the spin vector, α, becomes random for each measurement, resulting in variation of $S_\perp = S\cos\alpha$. The change of α corresponds to adding the phase $-m\alpha$ to each Φ_m. In addition, α fluctuates due to the temporal fluctuation of the magnetic bias field.

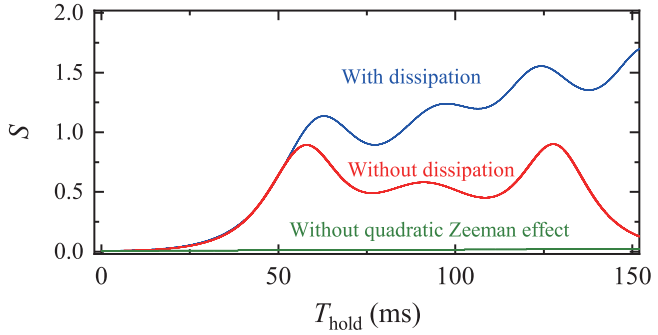

FIG. 3: Evolution of the magnetization from numerical simulation. The blue and red curves are obtained by solving the 3D GP equation with and without the dissipation of atoms, respectively. In the green curve, the quadratic Zeeman effect is excluded.

We evaluate the magnitude of S that best fits the 60 experimental data points of $|S_\perp|$ obtained during $T_{\rm hold}$ = 120–150 ms in Fig. 2(c). When S reaches a certain value and assuming α is random and uniform over $[0, 2\pi]$, the probability distribution of $|S_\perp|$ is represented by $p(|S_\perp|) \propto (S^2 - |S_\perp|^2)^{-1/2}$, where $0 \le |S_\perp| \le S$. The red outline histogram in Fig. 2(d) shows $p(|S_\perp|)$ integrated within the bin width for $S = 1.9$.

We perform three-dimensional numerical simulations of the Gross-Pitaevskii (GP) equation (see SM). Figure 3 shows a typical example of the time evolution of the transverse magnetization S. Magnetization is never produced under a condition of zero magnetic field, corresponding to the green curve in Fig. 3. When the quadratic Zeeman energy is included, as shown by the red curve, the magnetization initially grows but then decreases. The magnitude of the magnetization is limited to no more than $S \simeq 1$, and thus this result disagrees with the experimental findings. The initial growth in the magnetization is due to the combined effect of the s-wave spin-exchange interaction and the quadratic Zeeman effect. The energies of the $m = \pm1$ and $m = \pm2$ states are lowered by the quadratic Zeeman energy $qm^2 (q < 0)$, and the transitions from the $m = 0$ state to these states are enhanced. The quadratic Zeeman effect also rotates Φ_m by $(qm^2/\hbar)t$, which results in temporal modulation of S. Thus, the quadratic Zeeman effect produces magnetization, but never synchronizes the phase Φ_m to enhance the magnetization.

Next we solve the GP equation by taking into account spin-dependent particle dissipation. As shown in the blue curve in Fig. 3, the increase in the magnetization up to $T_{\rm hold} \simeq 60$ ms is similar to that for the case without par-

ticle dissipation. Unlike the non-dissipative system, the magnetization in the dissipative system continues to increase, which is in qualitative agreement with the experimental result in Fig. 2. This result indicates that the growth of magnetization after $T_{\rm hold} \simeq 60$ ms is driven mainly by the spin-dependent dissipation. However, the blue curve in Fig. 3 does not reach the values of $S \simeq 1.9$ obtained in Fig. 2(d), which may be due to effects not taken into account in the simulations, such as thermal effects [22].

The growth of magnetization by particle dissipation is described by the spin-dependent part of the energy:

$$E_{\rm spin} = \int d\boldsymbol{r} \left(\frac{g_4 - g_2}{14} \boldsymbol{s} \cdot \boldsymbol{s} + \frac{7g_0 - 10g_2 + 3g_4}{14} |A_0|^2 \right), \quad (1)$$

where $g_{\mathcal{F}}$ is the interaction coefficient for the colliding channels of total spins $\mathcal{F} = 4$, 2, and 0; $\boldsymbol{s}$ is the magnetization density; and $|A_0|$ is the spin-singlet density. The spin-dependent particle dissipation is expressed by the non-positive imaginary part of the interaction coefficient $g_{\mathcal{F}}$ [12]. The imaginary part of the first term represents the relative enhancement or suppression of the magnetization, depending on its sign. As mentioned above, decay through the $\mathcal{F} = 4$ channel is prohibited ($\mathrm{Im}g_4 = 0$) and the imaginary part of the coefficient of $\boldsymbol{s} \cdot \boldsymbol{s}$ is always non-negative, which enhances $|\boldsymbol{s}|$ relative to the total density. The magnetized state is thus more likely to survive than any other state under spin-dependent particle dissipation, which leads to the formation of the ferromagnetic eigenstate. In other words, spin-dependent dissipation assists the synchronization of Φ_m to promote the transverse magnetization. This is quite different from the phase decoherence due to the dissipative environment; the present effect of dissipation protects the specific eigenstate.

From the form of Eq. (1), we find that the singlet-pair density $|A_0|$ is also enhanced or suppressed by the spin-dependent particle dissipation, which suggests that other magnetic eigenstates can emerge depending on the values of Im $g_{\mathcal{F}}$. One such eigenstate is the cyclic state, which is a BEC of singlet trios of spin-2 atoms [11, 19–21]. The cyclic state emerges when the singlet-pair density $|A_0|$ and the magnetization $|\boldsymbol{s}|$ are both suppressed. As mentioned above, the imaginary part of $g_4 - g_2$ in Eq. (1) is always non-negative, which causes $|\boldsymbol{s}|$ to increase. However, if $|A_0|$ decreases before $|\boldsymbol{s}|$ grows, the cyclic state can be formed. This is achieved when $|\mathrm{Im}g_0|$ is large and $|\mathrm{Im}g_2|$ is small. Figure 4 shows the time evolution of $|\boldsymbol{s}|$ and $|A_0|$ for such a case for $\mathrm{Im}g_0$ and $\mathrm{Im}g_2$. The initial state is $\hat{R}_x(\pi/2)|2, 0\rangle$. The blue curve in Fig. 4 shows that $|A_0|$ decays to almost zero in the presence of particle dissipation while $|\boldsymbol{s}|$ remains small, indicating that the cyclic state is formed. The spherical harmonic representations of the spin states also show that the initial polar state evolves into the cyclic state, as shown in the inset of Fig. 4. It is notable that such tetrahedral symmetry arises from particle dissipation. Both the initial state and the cyclic state have populations in the $m = 0$ and $m = \pm 2$ states, with relative phases of $\phi_2 + \phi_{-2} - 2\phi_0 = 0$ for the initial state and π for the cyclic state. Thus the spin-dependent particle dissipation also affects the phases Φ_m in the generation of the cyclic state.

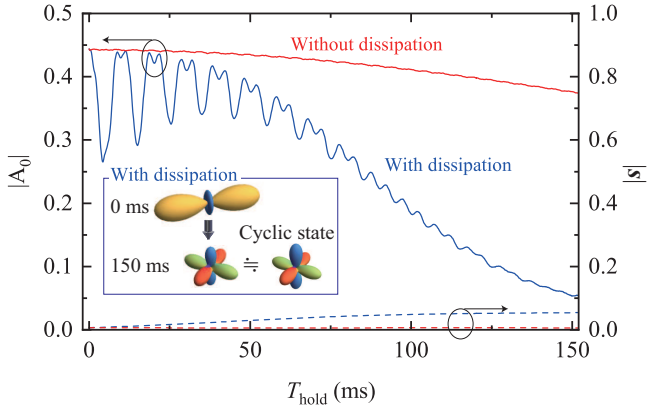

FIG. 4: Formation of the cyclic state (magnetic eigenstate). Numerical simulation of the time evolution of $|A_0|$ and $|\boldsymbol{s}|$, when $\mathrm{Im}g_0$ and $\mathrm{Im}g_2$ are ten times and one-tenth their values for ^{87}Rb, respectively. The initial spin state is $\hat{R}_x(\pi/2)\,|2, 0\rangle$. The size of the magnetic field, B_z, is 50 mG. The spherical harmonic representations of the spin states at the centre of the condensate are shown in the insets (see Supplemental Material).

We have experimentally and theoretically investigated the role of dissipation in a BEC of spin-2 ^{87}Rb atoms and found that particle dissipation can give rise to quantum coherence. Although the interactions between the atomic spins are not ferromagnetic, we nonetheless observed the emergence of transverse magnetization, in which the relative phases among the five magnetic sublevels are synchronized. Numerical simulations revealed that this phenomenon is mainly due to spin-dependent particle dissipation. It has also been shown that with appropriate loss parameters, such dissipation can lead to the formation of a cyclic magnetic state. These results indicate that naturally occurring dissipation gives rise to robustness of quantum coherence.

This work was supported by JSPS KAKENHI (grant nos. JP17K05595, JP17K05596, JP16K05505, JP15K05233, and JP25103007) and JST PRESTO (grant no. JPMJPR17G3). Y.E. acknowledges support from the Leading Initiative for Excellent Young Researchers (LEADER).

[1] M. A. Nielsen, and I. L. Chuang, *Quantum Computation and Quantum Information* (Cambridge Univ. Press, 2000).

[2] F. Verstraete, M. M. Wolf, J. I. Cirac, Quantum computation and quantum-state engineering driven by dissipation, Nature Phys. **5,** 633-636 (2009).

[3] S. Diehl, A. Micheli, A. Kantian, B. Kraus, H. P. Büchler, P. Zoller, Quantum states and phases in driven open quantum systems with cold atoms, Nature Phys. **4,** 878-883 (2008).

[4] S. Shankar, M. Hatridge, Z. Leghtas, K. M. Sliwa, A. Narla, U. Vool, S. M. Girvin, L. Frunzio, M. Mirrahimi, M. H. Devoret, Autonomously stabilized entanglement between two superconducting quantum bits, Nature **504,** 419-422 (2013).

[5] Y. Lin, J. P. Gaebler, F. Reiter, T. R. Tan, R. Bowler, A. S. Sørensen, D. Leibfried, D. J. Wineland, Dissipative production of a maximally entangled steady state of two quantum bits, Nature **504,** 415-418 (2013).

[6] T. Tomita, S. Nakajima, I. Danshita, Y. Takasu, Y. Takahashi, Observation of the Mott insulator to superfluid crossover of a driven-dissipative Bose-Hubbard system, Sci. Adv. **3,** e1701513 (2017).

[7] D. F. Walls, and G. J. Milburn, *Quantum Optics* (Springer-Verlag, Berlin, 1994).

[8] N. Lambert, Y.-N. Chen, Y.-C. Cheng, C.-M. Li, G.-Y. Chen, Franco Nori, Quantum biology, Nature Phys. **9,** 1018 (2013).

[9] G. S. Engel, T. R. Calhoun, E. L. Read, T.-K. Ahn, T. Mančal, Y.-C. Cheng, R. E. Blankenship, G. R. Fleming, Evidence for wavelike energy transfer through quantum coherence in photosynthetic systems, Nature **446,** 782786 (2007).

[10] A. Ishizaki, G. R. Fleming, Theoretical examination of quantum coherence in a photosynthetic system at physiological temperature, Proc. Natl. Acad. Sci. USA **106,** 17255-17260 (2009).

[11] N. N. Klausen, J. L. Bohn, C. H. Greene, Nature of spinor Bose-Einstein condensates in rubidium, Phys. Rev. A **64,** 053602 (2001).

[12] S. Tojo, T. Hayashi, T. Tanabe, T. Hirano, Y. Kawaguchi, H. Saito, M. Ueda, Spin-dependent inelastic collisions in spin-2 Bose-Einstein condensates, Phys. Rev. A **80**, 042704 (2009).

[13] L. E. Sadler, J. M. Higbie, S. R. Leslie, M. Vengalattore, D. M. Stamper-Kurn, Spontaneous symmetry breaking in a quenched ferromagnetic spinor Bose-Einstein condensate, Nature **443,** 312-315 (2006).

[14] H. Schmaljohann, M. Erhard, J. Kronjäger, M. Kottke, S. van Staa, L. Cacciapuoti, J. J. Arlt, K. Bongs, K. Sengstock, Dynamics of $F = 2$ Spinor Bose-Einstein Condensates, Phys. Rev. Lett. **92,** 040402 (2004).

[15] M.-S. Chang, C. D. Hamley, M. D. Barrett, J. A. Sauer, K. M. Fortier, W. Zhang, L. You, M. S. Chapman, Observation of Spinor Dynamics in Optically Trapped ^{87}Rb Bose-Einstein Condensates Phys. Rev. Lett. **92,** 140403 (2004).

[16] T. Kuwamoto, K. Araki, T. Eno, T. Hirano, Magnetic field dependence of the dynamics of ^{87}Rb spin-2 Bose-Einstein condensates, Phys. Rev. A **69,** 063604 (2004).

[17] C. S. Gerving, T. M. Hoang, B. J. Land, M. Anquez, C. D. Hamley, M. S. Chapman, Non-equilibrium dynamics of an unstable quantum pendulum explored in a spin-1 BoseEinstein condensate, Nature Comm. **3,** 1169 (2012).

[18] Y. Eto, M. Sadgrove, S. Hasegawa, H. Saito, and T. Hirano, Control of spin current in a Bose gas by periodic application of π pulses, Phys. Rev. A **90,** 013626 (2014).

[19] M. Koashi, M. Ueda, Exact Eigenstates and Magnetic Response of Spin-1 and Spin-2 Bose-Einstein Condensates, Phys. Rev. Lett. **84,** 1066 (2000).

[20] C. V. Ciobanu, S.-K. Yip, T.-L. Ho, Phase diagrams of $F = 2$ spinor Bose-Einstein condensates, Phys. Rev. A **61,** 033607 (2000).

[21] M. Ueda, M. Koashi, Theory of spin-2 Bose-Einstein condensates: Spin correlations, magnetic response, and excitation spectra, Phys. Rev. A **65,** 063602 (2002).

[22] H. Schmaljohann, M. Erhard, J. Kronjäger, K. Sengstock, and K. Bongs Dynamics and thermodynamics in spinor quantum gases, Appl. Phys. B **79,** 1001 (2004).

[23] See Supplemental Material [url] for experimental and theoretical details, which includes Refs. [24-28].

[24] M. Sadgrove, Y. Eto, S. Sekine, H. Suzuki, and T. Hirano, Ramsey interferometry using the Zeeman sublevels in a spin-2 Bose gas, J. Phys. Soc. Jpn. **82,** 094002 (2013).

[25] A. Widera, F. Gerbier, S. Fölling, T. Gericke, O. Mandel, I. Bloch, Precision measurement of spin-dependent interaction strengths for spin-1 and spin-2 ^{87}Rb atoms, New J. Phys. **8**, 152 (2006).

[26] W. H. Press, S. A. Teukolsky, W. T. Vetterling, and B. P. Flannery, *Numerical Recieps*, 3rd ed. (Cambridge Univ. Press, Cambridge, 2007).

[27] M. J. Steel, M. K. Olsen, L. I. Plimak, P. D. Drummond, S. M. Tan, M. J. Collett, D. F. Walls, and R. Graham, Dynamical quantum noise in trapped Bose-Einstein condensates, Phys. Rev. A **58**, 4824 (1998).

[28] J. D. Sau, S. R. Leslie, D. M. Stamper-Kurn, and M. L. Cohen, Theory of domain formation in inhomogeneous ferromagnetic dipolar condensates within the truncated Wigner approximation, Phys. Rev. A **80**, 023622 (2009).